

Metal substituents can be used to tune the physical properties of these Li-rich phases because they affect the $(\text{O}_2)^{n-}$ stability against oxygen recombination or voltage fade, as previously demonstrated for $\text{Li}_2\text{Ru}_{1-x}\text{M}_x\text{O}_3$ ($\text{M} = \text{Sn}, \text{Ti}, \text{Mn}$). The benefits of Sn, in that it limits both $\text{O}_{2(g)}$ release and voltage fade, are preserved in the $\text{Li}_2\text{Ir}_{1-y}\text{Sn}_y\text{O}_3$ system but are mitigated by the emergence of a capacity fade mechanism that is linked to the emergence and accumulation of stacking faults. This finding emphasizes that the origins of voltage and capacity fading in these Li-rich layered phases are different, a point that has previously been a source of confusion.

In summary, combined TEM, neutron diffraction, and ab initio studies on high-capacity Li-rich $\text{Li}_2\text{Ir}_{1-x}\text{Sn}_x\text{O}_3$ layered phases permitted the atomic-scale visualization of the $(\text{O}-\text{O})^{n-}$ peroxo-like dimers responsible for the capacity gain in Li-rich layered electrode materials. These observations lead to a better understanding of peroxo formation and localization, O_2 recombination, and the effect of the transition metal substituents. Additionally, these findings provide a chemical handle for tuning the performances of Li-rich layered materials.

REFERENCES AND NOTES

- B. L. Ellis, K. T. Lee, L. F. Nazar, *Chem. Mater.* **22**, 691–714 (2010).
- Z. Lu, L. Y. Beaulieu, R. A. Donaberg, C. L. Thomas, J. R. Dahm, *J. Electrochem. Soc.* **149**, A778 (2002).
- M. M. Thackeray, C. S. Johnson, J. T. Vaughey, N. Li, S. A. Hackney, *J. Mater. Chem.* **15**, 2257–2267 (2005).
- J. M. Tarascon et al., *J. Solid State Chem.* **147**, 410–420 (1999).
- G. Ceder et al., *Nature* **392**, 694–696 (1998).
- M. K. Aydinol, A. F. Kohan, G. Ceder, K. Cho, J. Joannopoulos, *Phys. Rev. B* **56**, 1354–1365 (1997).
- C.-C. Chang, O. I. Veikokhatnyi, P. N. Kumta, *J. Electrochem. Soc.* **151**, J91–J94 (2004).
- J. Graetz, C. C. Ahn, R. Yazami, B. Fultz, *J. Phys. Chem. B* **107**, 2887–2891 (2003).
- S. Laha et al., *Phys. Chem. Chem. Phys.* **17**, 3749–3760 (2015).
- H. Koga et al., *J. Phys. Chem. C* **118**, 5700–5709 (2014).
- M. Oishi et al., *J. Power Sources* **276**, 89–94 (2015).
- W.-S. Yoon et al., *J. Phys. Chem. B* **106**, 2526–2532 (2002).
- M. Sathiyar et al., *Nat. Mater.* **12**, 827–835 (2013).
- M. Sathiyar et al., *Nat. Mater.* **14**, 230–238 (2015).
- M. Sathiyar et al., *Chem. Mater.* **25**, 1121–1131 (2013).
- E. McCalla et al., *J. Electrochem. Soc.* **162**, A1341–A1351 (2015).
- J. Rouxel, *Chem. Eur. J.* **2**, 1053–1059 (1996).
- M. Sathiyar et al., *Chem. Commun.* **49**, 11376–11378 (2013).
- E. McCalla et al., *J. Am. Chem. Soc.* **137**, 4804–4814 (2015).
- A. R. Armstrong et al., *J. Am. Chem. Soc.* **128**, 8694–8698 (2006).
- N. Yabuuchi et al., *Proc. Natl. Acad. Sci. U.S.A.* **112**, 7650–7655 (2015).
- Materials and methods are available as supplementary materials on Science Online.
- H. Kobayashi, M. Tabuchi, M. Shikano, H. Kageyama, R. Kanno, *J. Mater. Chem.* **13**, 957–962 (2003).
- S. D. Findlay et al., *Ultramicroscopy* **110**, 903–923 (2010).
- R. Ishikawa et al., *Nat. Mater.* **10**, 278–281 (2011).
- L. Gu, D. Xiao, Y.-S. Hu, H. Li, Y. Ikuhara, *Adv. Mater.* **27**, 2134–2149 (2015).
- D. Batuk, M. Batuk, A. M. Abakumov, J. Hadernann, *Acta Crystallogr. B* **71**, 127–143 (2015).
- S.-C. Yin, Y. H. Rho, I. Swainson, L. F. Nazar, *Chem. Mater.* **18**, 1901–1910 (2006).
- F. Grasset, C. Dussarrat, J. Darriet, *J. Mater. Chem.* **7**, 1911–1915 (1997).
- M. Sathiyar et al., *Nat. Commun.* **6**, 6276 (2015).
- J. Lee et al., *Science* **343**, 519–522 (2014).

ACKNOWLEDGMENTS

E.M. thanks the Fonds de Recherche du Québec-Nature et Technologies and ALISTORE-European Research Institute for funding this work, as well as the European community I3 networks for funding the neutron scattering research trip. This work was also funded by the Slovenian Research Agency research program P2-0148. This work is partially based on experiments performed at the Institut Laue Langevin. We thank J. Rodriguez-Carvajal for help with neutron scattering experiments and for fruitful discussions. We also thank M. T. Sougrati for performing the Sn-Mössbauer measurements. Use of the Advanced Photon Source at Argonne National Laboratory was supported

by the U.S. Department of Energy, Office of Science, Office of Basic Energy Sciences, under contract no. DE-AC02-06CH11357. M.S. and M.-L.D. acknowledge high-performance computational resources from GENCI-CCRT/CINES (grant cmm6691). J.-M.T. acknowledges funding from the European Research Council (ERC) (FP/2014-2020)/ERC Grant-Project670116-ARPEMA.

SUPPLEMENTARY MATERIALS

www.sciencemag.org/content/350/6267/1516/suppl/DC1
Materials and Methods
Figs. S1 to S13
Tables S1 and S2
References (32–43)

19 June 2015; accepted 6 November 2015
10.1126/science.aac8260

PLANT SYMBIOSES

Rice perception of symbiotic arbuscular mycorrhizal fungi requires the karrikin receptor complex

Caroline Gutsch, ^{1,2*} Enrico Gobbato, ^{3*} Jeongmin Choi, ³ Michael Riemann, ^{4,5} Matthew G. Johnston, ³ William Summers, ³ Samy Carbonnel, ² Catherine Mansfield, ³ Shu-Yi Yang, ¹ Marina Nadal, ¹ Ivan Acosta, ⁶ Makoto Takano, ⁴ Wen-Biao Jiao, ⁶ Korbinian Schneeberger, ⁶ Krystyna A. Kelly, ³ Uta Paszkowski ^{1,3†}

In terrestrial ecosystems, plants take up phosphate predominantly via association with arbuscular mycorrhizal fungi (AMF). We identified loss of responsiveness to AMF in the rice (*Oryza sativa*) mutant *hebiba*, reflected by the absence of physical contact and of characteristic transcriptional responses to fungal signals. Among the 26 genes deleted in *hebiba*, *DWARF 14 LIKE* is, the one responsible for loss of symbiosis. It encodes an alpha/beta-fold hydrolase, that is a component of an intracellular receptor complex involved in the detection of the smoke compound karrikin. Our finding reveals an unexpected plant recognition strategy for AMF and a previously unknown signaling link between symbiosis and plant development.

Most land plants establish symbioses with arbuscular mycorrhizal fungi (AMF) of the phylum *Glomeromycota* (1). These symbioses contribute to global carbon and mineral nutrient cycles, because AMF provide mineral nutrients to the plant and receive carbohydrates in return. Colonization of plant roots by AMF requires reciprocal recognition initiated by diffusible molecules before fungal

attachment to the root surface and root penetration via hyphopodia (2). Diffusible precolonization signals include strigolactones, released from plant roots that activate the fungus before physical interaction (3), and fungal (lipo)chitooligosaccharides and chitotetraose, secreted by AMF that trigger plant calcium signaling, gene expression, and lateral root formation (4, 5). Plant LysM receptor-like kinases (6) are required for perception of chitinaceous microbial molecules that trigger either symbiosis or defense signaling (7–9). Plant signaling mutants impaired in root colonization by both AMF and nitrogen-fixing bacteria still exhibit transcriptional responses to fungal signaling molecules (10–12). Therefore, additional signaling modules have been postulated (12). We identified the rice receptor for karrikin, a plant growth regulator first identified in smoke (13–16), as a necessary signaling component for establishment of arbuscular mycorrhizal (AM) symbiosis.

We found that the jasmonate-deficient rice (*Oryza sativa*) mutant *hebiba* (17) was unable to

¹Department of Plant Molecular Biology, University of Lausanne, Biophore Building, 1015 Lausanne, Switzerland.
²Faculty of Biology, Genetics, University of Munich, Biocenter Martinsried, Grosshaderner Straße 2-4, 82152 Martinsried, Germany.
³Department of Plant Sciences, University of Cambridge, Downing Street, Cambridge CB2 3EA, UK.
⁴Division of Plant Sciences, National Institute of Agrobiological Sciences, 2-1-2 Kannondai, Tsukuba, Ibaraki 305-8602, Japan.
⁵Botanical Institute, Molecular Cell Biology, Karlsruhe Institute of Technology, Kaiserstraße 2, 76131 Karlsruhe, Germany.
⁶Max Planck Institute for Plant Breeding Research, Carl-von-Linné-Weg 10, D-50829 Cologne, Germany.

*These authors contributed equally to this work.

†Corresponding author. E-mail: up220@cam.ac.uk

establish symbiosis with either of two AMF—*Rhizophagus irregularis* and *Gigaspora rosea*—as reflected by the absence of hyphopodia, intraradical colonization, and induction of colonization marker genes (Fig. 1, A to C) (10). The lack of fungal interaction persisted upon increased inoculum strength imposed by growing *hebiba* alongside colonized wild-type plants (Fig. 1D). This suggested that the mutant is compromised at a very early stage of the interaction, during pre-symbiotic signaling.

The *hebiba* mutant is due to a genomic deletion of 169 kb, which contains 26 annotated genes (17, 18). One of the genes encodes allene oxide cyclase (AOC), part of the jasmonate biosynthetic pathway, loss of which leads to jasmonate deficiency (17). However, transgenic complementation of *hebiba* with *AOC* (*hebiba*^{AOC}) did not restore AM symbiosis (fig. S1) (17, 19). Therefore, another gene contained within the deleted interval must be required for AM development.

We identified the gene responsible for AM symbiosis by transforming *hebiba*^{AOC} with genomic clones of individual genes from the deleted interval (table S1) (17, 18). Reintroduction of the *LOC_Os03g32270* gene restored fungal colonization of *hebiba*^{AOC} roots in independent rice transformants (Fig. 2, A and B, and table S1).

Quantitative measurements of colonization correlated ($R^2 = 0.84$) with the amount of transcript accumulation from the *LOC_Os03g32270* transgene (Fig. 2C). Transgenic lines such as C10 (Fig. 2B), with transgene mRNA levels below the detection limit, retained the *hebiba* mutant phenotype. *LOC_Os03g32270* encodes the alpha/beta-fold hydrolase DWARF14LIKE (D14L), homologous to *Arabidopsis thaliana* KARRIKIN INSENSITIVE2/HYPOSENSITIVE TO LIGHT (KAI2/HTL). This hydrolase acts together with the F-box protein DWARF3/MORE AXILLARY GROWTH2 (D3/MAX2) in the perception of karrikins, a group of butenolide compounds found in smoke that induce seed germination in fire-chasing plants (13–16). The structurally related strigolactones are perceived by a receptor complex involving D3 and the alpha/beta-fold hydrolase DWARF14 (D14), the paralog of D14L (20–22). However, the strigolactone-insensitive rice mutant *d14* is not perturbed in AM symbiosis (23) (Fig. 3A); thus, the strigolactone receptor gene *D14* is not required for establishment of the interaction. A rice *d3* mutant was also severely impaired in AM colonization and marker gene induction (Fig. 3, A and B) (23), revealing the importance of the karrikin receptor complex for the earliest stages of AM development. We further confirmed the requirement of D14L in AM development by using a set

of RNA interference (RNAi) lines generated in the *Oryza sativa* cv. Nipponbare background. The RNAi lines displayed diverse levels of AM suppression that correlated ($R^2 = 0.69$) with the degree of down-regulation of endogenous *LOC_Os03g32270* (fig. S2, A to C). The *D14L* RNAi line Ri43 supports AMF colonization (23); however, we found a decrease ($P = 0.047$) in total fungal colonization relative to wild type in this line. The phenotypic diversity among the *D14L* RNAi lines suggests a low transcript threshold for AM symbiosis establishment.

In *Arabidopsis*, *KAI2/HTL* controls hypocotyl elongation in response to light and karrikin (13, 24). Overexpression of rice *D14L* in an *Arabidopsis htl-2* mutant restored wild-type hypocotyl length in two independent F₃ populations homozygous for *htl-2* (fig. S3A). Mesocotyl elongation assays in rice demonstrated that *hebiba*^{AOC} is insensitive to karrikin but responds to the synthetic strigolactone GR24 (fig. S3B). In contrast, mutations of *D14* specifically compromised strigolactone but not karrikin responses in rice, whereas mutation of the F-box protein encoding *D3* resulted in insensitivity to both (fig. S3B). Thus, in rice, D14L and D14 mediate perception specificity to karrikin versus strigolactone in an overall similar manner to *Arabidopsis* (13). However, the partial response of *Arabidopsis d14* to racemic

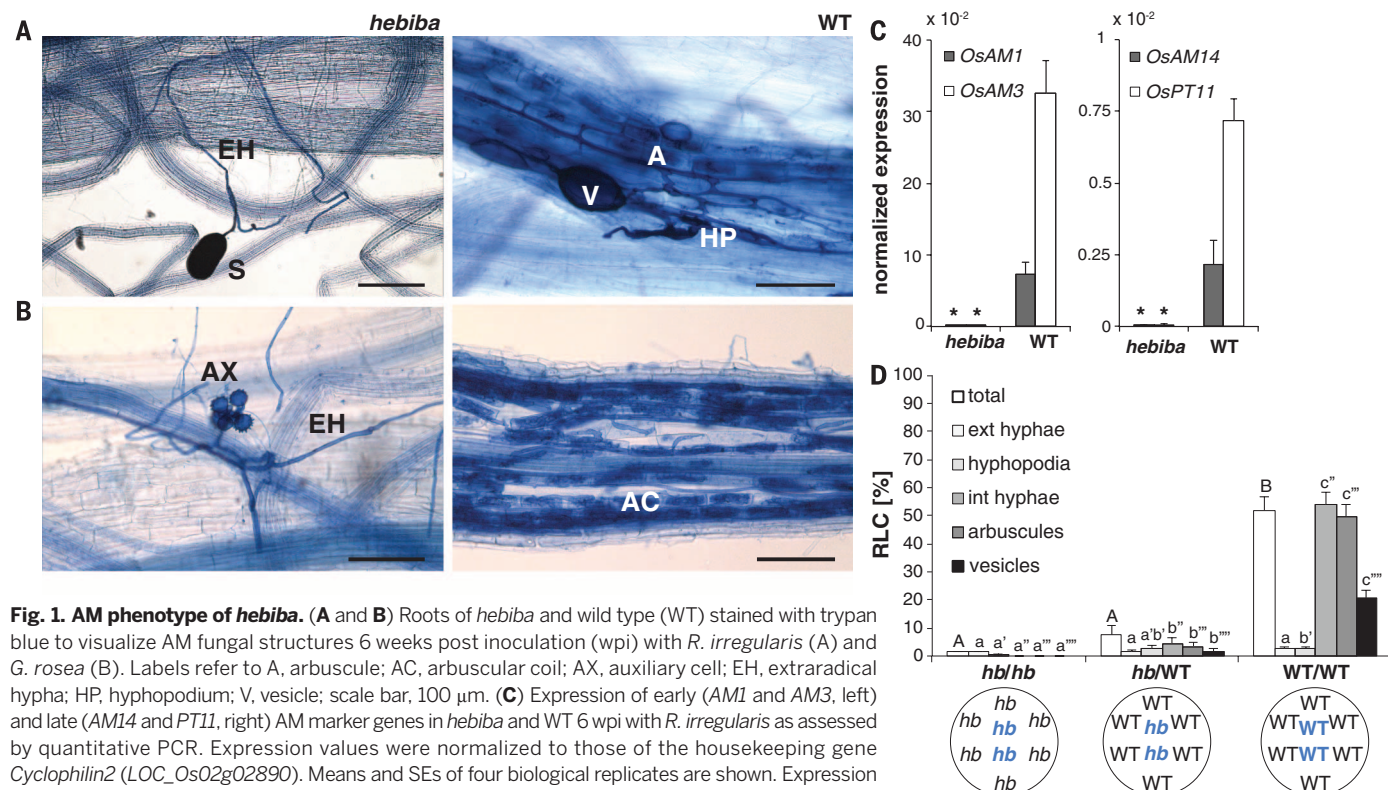


Fig. 1. AM phenotype of *hebiba*. (A and B) Roots of *hebiba* and wild type (WT) stained with trypan blue to visualize AM fungal structures 6 weeks post inoculation (wpi) with *R. irregularis* (A) and *G. rosea* (B). Labels refer to A, arbuscule; AC, arbuscular coil; AX, auxiliary cell; EH, extraradical hypha; HP, hyphopodium; V, vesicle; scale bar, 100 μ m. (C) Expression of early (*AM1* and *AM3*, left) and late (*AM14* and *PT11*, right) AM marker genes in *hebiba* and WT 6 wpi with *R. irregularis* as assessed by quantitative PCR. Expression values were normalized to those of the housekeeping gene *Cyclophilin2* (*LOC_Os02g02890*). Means and SEs of four biological replicates are shown. Expression was significantly less in *hebiba* than WT ($P = 0.02$ for each gene; Kruskal-Wallis test with Benjamini-Hochberg adjustment for multiple testing). (D) Percentage of root length colonization (RLC) by *R. irregularis* of two central “tester” surrounded by six “donor” plants at 7 wpi. Means and standard errors of five biological replicates are shown. ext hyphae, extraradical hyphae; int hyphae, intraradical hyphae. For each of the six fungal structures in the figure, separate Kruskal-Wallis tests were performed, using the Benjamini-Hochberg adjustment for the post hoc tests. The P values were as follows: P (total) ≤ 0.01 , P (ext. hyphae) = 0.43, P (hyphopodia) ≤ 0.05 , P (int. hyphae, arbuscules, vesicles) ≤ 0.001 . The letters above each bar indicate growth conditions that were not significantly different in the post hoc pairwise comparisons. The comparisons are for bars with the same case and number of apostrophes.

GR24 (13, 25) was not reproduced in rice *d14* mutants (fig. S3B) (26), suggesting that D14L has less redundant activity in rice. Fluorescently tagged D14L in *Arabidopsis* (24) and rice localized to both nucleus and cytoplasm (Fig. 2E). D14L in rice (Fig. 2D) as in *Arabidopsis* (24) is expressed in all rice organs, and transcript accumulation in roots is not altered during AM colonization.

We asked whether D14L is required for suppression of defense responses against AMF. We found no evidence for increased activation of selected defense marker genes (27) during the early stages of mycorrhizal colonization (fig. S4, A and B). Moreover, *hebiba*^{AOC} was susceptible to colonization by the root endophyte *Piriformospora indica* and the pathogen *Magnaporthe oryzae* (fig. S4, C and D), implicating D14L in symbiotic compatibility.

On the basis of the early and pronounced *hebiba* mutant phenotype, we hypothesized that functional D14L is required for the perception of AM fungi before contact. Germinated spore exudates (GSEs) of AMF activate precontact plant responses (28). Therefore, we used RNA sequencing

(RNA-seq) to monitor the transcriptional changes of *hebiba*^{AOC} and wild-type roots in response to GSEs over the first 24 hours post treatment (hpt) (supplementary materials, tables S2 and S3). Overall 140 genes showed statistically significant differences in average expression upon GSE treatment in wild-type plants (Fig. 4A and tables S4 and S5). In *hebiba*^{AOC} plants, six genes responded significantly to GSEs, of which two genes (predicted to encode an expressed and a hypothetical protein) overlapped with the genes responding in wild type (Fig. 4A and table S4), suggesting that the transcriptional response observed in the wild-type relied on functional D14L. Time-resolved gene ontology (GO) analyses of genes differentially regulated in response to GSEs in wild type but not in *hebiba*^{AOC} demonstrated an overrepresentation of terms associated with responses to extracellular and biotic stimuli. Genes were induced or repressed at the earliest time points, 3 and 6 hpt, and in a *D14L*-dependent fashion, consistent with D14L playing a role in early signaling activation (Fig. 4B and table S6, A and B). The expression pattern of

representative genes was validated by quantitative reverse transcription polymerase chain reaction (RT-PCR) on the same RNA used for the RNA-seq experiment (fig. S5A) and on RNA from two additional biological replicates, which included the complemented line C11 (fig. S5B). Thus, D14L is required to support initial colonization events by AMF. Despite its effect on mesocotyl elongation, treatment with karrikin did not induce significant gene expression changes in roots of wild-type rice (table S4). Also, the exogenous application of karrikin did not stimulate colonization of wild-type roots by *R. irregularis* (fig. S6).

We found that a total of 104 transcripts differed significantly between untreated *hebiba*^{AOC} and wild-type roots (table S4) derived from genes with borderline GO-term enrichment for metabolic processes (table S6C). Whereas mRNA levels of known genes essential for AM symbiosis accumulated independently of functional D14L, transcript levels of the rice homolog of *DWARF14 LIKE 2* (13), *LOC_Os05g51240*, depended on D14L, as earlier observed in *Arabidopsis* (13) (table S4). In

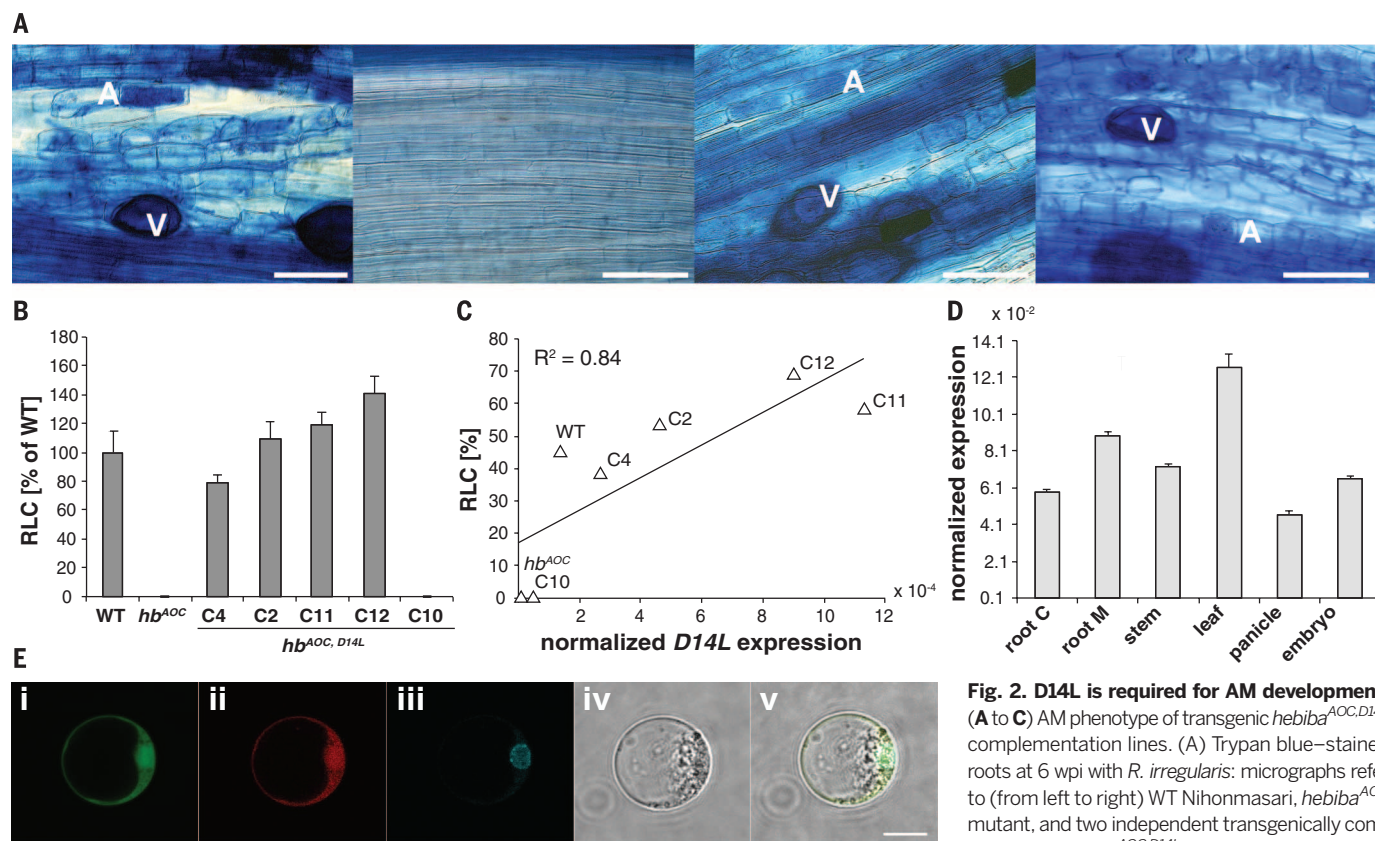


Fig. 2. D14L is required for AM development.

(A to C) AM phenotype of transgenic *hebiba*^{AOC,D14L} complementation lines. (A) Trypan blue-stained roots at 6 wpi with *R. irregularis*; micrographs refer to (from left to right) WT Nihonmasari, *hebiba*^{AOC} mutant, and two independent transgenically complemented *hebiba*^{AOC,D14L} lines (C4 and C11). Scale

bar, 50 μ m. (B) RLC expressed as % of WT colonization at 6 wpi for independent *hebiba*^{AOC,D14L} complementation lines. Values represent means and SEs from two to five replicate plants. (C) *D14L* transcript levels were assessed by real-time RT-PCR in the independent transgenic complementation lines. The averages for the WT, *hebiba*^{AOC}, and the complementation *hebiba*^{AOC,D14L} lines were plotted against the corresponding averages for total RLC. The Spearman rank correlation was calculated and squared to give the proportion of the variation accounted for by the correlation. (D) Real-time RT-PCR-based expression of *D14L* in control root (C), mycorrhizal roots (M), stem, leaf, panicle, and embryo of Nipponbare rice. Expression values were normalized to those of the constitutively expressed gene *Cyclophilin2* (*LOC_Os02g02890*). Means and SDs of three technical replicates are shown. (E) Subcellular localization of D14L. A plasmid containing a *D14L* overexpression construct (i) maize ubiquitin promoter:*D14L* cDNA:green fluorescent protein was co-transfected with the plasmid containing a genomic clone of *D14L* driven by its native promoter (ii) p*D14L*:g*D14L*:RFP in rice root protoplasts. (iii) DAPI staining. (v) Overlay of all channels, including bright field (iv). Scale bar, 10 μ m.

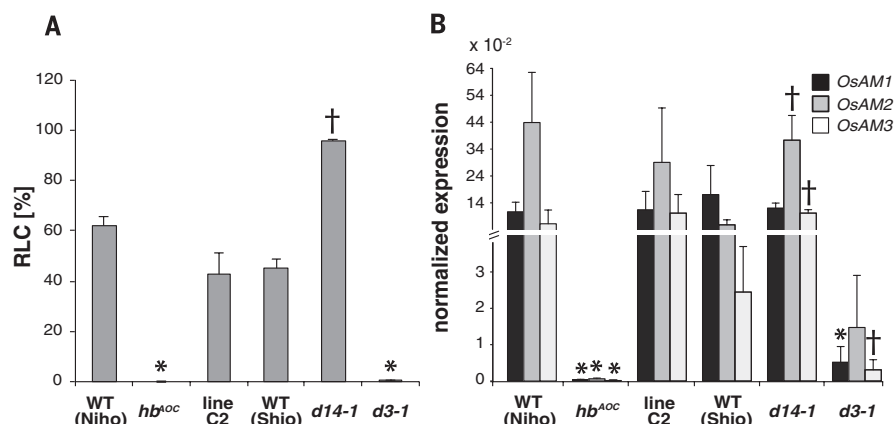


Fig. 3. AM phenotype of d3 relative to *hebiba*^{AOC}, d14, and corresponding WT cultivars. (A) Percentage of RLC and (B) induction of AM early marker genes at 7 wpi with *R. irregularis* of d3, d14, *hebiba*^{AOC}, *hebiba*^{AOC,d14L} complementation line C2, and corresponding WT background Nihonmasari (Niho) and Shiokari (Shio), respectively. Expression values were normalized to those of the constitutively expressed gene *Cyclophilin2* (*LOC_Os02g02890*). Values represent means and SEs from three biological replicates (A and B). The mutants and complementation line were compared with the appropriate WT by using the Kruskal-Wallis test. Symbols above the bars indicate statistical significance with respect to the WT (†*P* < 0.10; **P* < 0.05).

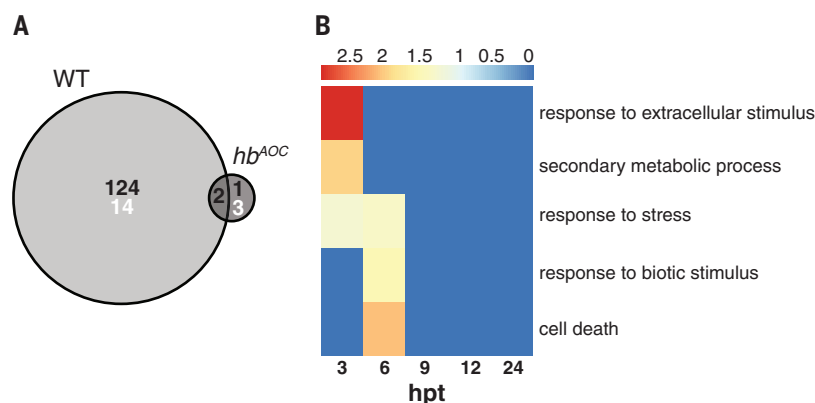


Fig. 4. GSE-induced transcriptional responses of WT and *hebiba*^{AOC}. (A) Venn diagram depicting the number of transcripts induced (black) and repressed (white) in WT and *hebiba*^{AOC} plants treated with GSEs in comparison to plants receiving a mock treatment. (B) Time-resolved GO-term enrichment analysis (*P* ≤ 0.001) for genes differentially regulated in response to GSEs in WT but not in *hebiba*^{AOC}. The color code represents odds ratios.

contrast to *Arabidopsis*, karrikin treatment of rice roots did not induce this gene. Because D14L is found in genomes of plants that germinate without fire stimulation and because *Arabidopsis* mutants lacking D14L show developmental phenotypes, we hypothesize that an endogenous ligand exists and is required for wild-type seedling development (29). In rice, the differences in transcriptomes between GSEs and mock or karrikin-treated wild-type plants indicate either that this ligand is not karrikin or that D14L acts upstream of the GSE response, thereby possibly creating a condition permissive for AM symbiosis.

We show that the karrikin receptor complex is central to the everyday interaction of plants with AMF, involving more than 80% of all plant species as opposed to 1200 smoke-responsive plant species (30). Conservation of D14L in early land plants, such as liverworts (31), suggests that

it has served this purpose since AMF started supporting terrestrial plant life. On poor natural soils, plants rely on AMF for mineral nutrient supply and need to coordinate AMF development with their physiological and developmental needs. The karrikin receptor complex may represent a node in the cross-talk between plant development and AM signaling.

REFERENCES AND NOTES

1. S. Smith, D. Read, *Mycorrhizal Symbiosis* (Academic Press, London, ed. 3, 2008).
2. C. Gutjahr, M. Parniske, *Annu. Rev. Cell Dev. Biol.* **29**, 593–617 (2013).
3. K. Akiyama, K. Matsuzaki, H. Hayashi, *Nature* **435**, 824–827 (2005).
4. F. Maillat *et al.*, *Nature* **469**, 58–63 (2011).
5. A. Genre *et al.*, *New Phytol.* **198**, 190–202 (2013).
6. C. Gough, J. Cullimore, *Mol. Plant Microbe Interact.* **24**, 867–878 (2011).
7. G. E. Oldroyd, *Nat. Rev. Microbiol.* **11**, 252–263 (2013).

8. X. Zhang *et al.*, *Plant J.* **81**, 258–267 (2015).
9. K. Miyata *et al.*, *Plant Cell Physiol.* **55**, 1864–1872 (2014).
10. C. Gutjahr *et al.*, *Plant Cell* **20**, 2989–3005 (2008).
11. C. Camps *et al.*, *New Phytol.* **208**, 224–240 (2015).
12. M. Nadal, U. Paszkowski, *Curr. Opin. Plant Biol.* **16**, 473–479 (2013).
13. M. T. Waters *et al.*, *Development* **139**, 1285–1295 (2012).
14. Y. Guo, Z. Zheng, J. J. La Clair, J. Chory, J. P. Noel, *Proc. Natl. Acad. Sci. U.S.A.* **110**, 8284–8289 (2013).
15. S. Toh, D. Holbrook-Smith, M. E. Stokes, Y. Tsuchiya, P. McCourt, *Chem. Biol.* **21**, 988 (2014).
16. G. R. Flematti, E. L. Ghisalberti, K. W. Dixon, R. D. Trengove, *Science* **305**, 977 (2004).
17. M. Riemann *et al.*, *Plant J.* **74**, 226–238 (2013).
18. K. J. V. Nordström *et al.*, *Nat. Biotechnol.* **31**, 325–330 (2013).
19. C. Gutjahr, H. Siegler, K. Haga, M. Iino, U. Paszkowski, *PLOS ONE* **10**, e0123422 (2015).
20. T. Arite *et al.*, *Plant Cell Physiol.* **50**, 1416–1424 (2009).
21. C. Hamiaux *et al.*, *Curr. Biol.* **22**, 2032–2036 (2012).
22. L.-H. Zhao *et al.*, *Cell Res.* **25**, 1219–1236 (2015).
23. S. Yoshida *et al.*, *New Phytol.* **196**, 1208–1216 (2012).
24. X.-D. Sun, M. Ni, *Mol. Plant* **4**, 116–126 (2011).
25. A. Scaffidi *et al.*, *Plant Physiol.* **165**, 1221–1232 (2014).
26. Z. Hu *et al.*, *Plant Cell Physiol.* **51**, 1136–1142 (2010).
27. S. Marcel, R. Sawers, E. Oakeley, H. Anglikier, U. Paszkowski, *Plant Cell* **22**, 3177–3187 (2010).
28. M. Chabaud *et al.*, *New Phytol.* **189**, 347–355 (2011).
29. M. T. Waters, A. Scaffidi, Y. K. Sun, G. R. Flematti, S. M. Smith, *Plant J.* **79**, 623–631 (2014).
30. S. D. S. Chivocha *et al.*, *Plant Sci.* **177**, 252–256 (2009).
31. P.-M. Delaux *et al.*, *New Phytol.* **195**, 857–871 (2012).

ACKNOWLEDGMENTS

We thank J. Gheyselinck for technical assistance; P. Nick (Karlsruhe Institute of Technology, Germany) for providing *hebiba* and Nihonmasari wild-type seeds; M. Nakazono (University of Nagoya, Japan) for providing d3 and Shiokari wild-type seeds; J. Kozuka (Graduate School of Agriculture and Life Sciences, University of Tokyo) for d14 seeds and the D14L RNAi line Ri43; and M. Ni (University of Minnesota, USA) for providing *Arabidopsis htl-2* seeds. T. Hardcastle helped by enhancing R/Bioconductor or package baySeq to enable the RNA-seq time course analysis. M. Meyer instructed the carbon-dioxide treatment of *R. irregularis*. C.G. received Ph.D. fellowships from the German National Academic Foundation (Studienstiftung des Deutschen Volkes), the Roche Research Foundation, and the German Research Council (DFG) (GU1423/1-1). E.G. was supported by the Isaac Newton Trust grant RG74108. J.C. is a European Molecular Biology Organization Long-Term Fellow (ALTF 117-2014), and W.S. is a UK Biotechnology and Biological Sciences Research Council–Doctoral Training Partnership scholar, supported by grant PDAG/223 T39. S.C. was funded by the Collaborative Research Center SFB924 “Molecular mechanisms regulating yield and yield stability in plants” of the German Research Council (DFG). Research in the U.P. laboratories was supported by the Swiss National Science Foundation “professeur boursier” grants PP00A-110874 and PP00P3-130704, and by the Gatsby Charitable Foundation grant RG60824. C.G., E.G., J.C., K.A.K., and U.P. designed the experiments. C.G., E.G., J.C., M.G.J., W.S., S.C., C.M., S.-Y.Y. M.N., and I.A. performed the experiments. K.A.K., W.-B.J., and K.S. performed bioinformatics and statistical analysis of the RNA-seq data. M.R. and M.T. provided access to unpublished mapping information. C.G., E.G., K.A.K., and U.P. wrote the manuscript. The supplementary materials contain additional data. The RNA-seq data have been deposited in ArrayExpress with accession number E-MTAB-4072. The authors declare no conflict of interest.

SUPPLEMENTARY MATERIALS

www.sciencemag.org/content/350/6267/1521/suppl/DC1
Materials and Methods
Figs. S1 to S6
Tables S1 to S7
References (32–49)

7 July 2015; accepted 16 November 2015
10.1126/science.aac9715